DOI: 10.24352/UB.OVGU-2017-115 TECHNISCHE MECHANIK, 37, 2-5, (2017), 394 – 399
submitted: June 15, 2017

On Behavior of a Double Rotor HAWT with a Differential Planet Gear

E. Shalimova, L. Klimina, K.-H. Lin

The mathematical model of a double disk horizontal axis wind turbine is constructed. The turbine has two propellers (actuator disks). One propeller is rigidly connected to a carrier of a planet gear, the other is rigidly connected to an external ring of the same planet gear. A rotor of an electrical generator is rigidly connected to a sun of the planet gear. The generator is included into a local electrical circuit with several consumers. The quasi-steady model of aerodynamic action is used. The electromechanical torque acting on the rotor of generator is assumed to be a linear function of an angular speed of the rotor. Existence and stability of steady motions are studied. Analysis of characteristics of steady motions such as angular speed of each propeller and mechanical power trapped from the flow is performed. A control strategy is suggested.

1 Introduction

Experimental tests and mathematical modeling have proved that using of two contra-rotating propellers in the construction of a horizontal axis wind turbine (HAWT) improves its aerodynamic characteristics (Jung et al., 2005; Shen et al., 2007; Farthing, 2010; Lee et al., 2012). Corresponding models of turbine aerodynamics are well-developed (see Hansen (2015)). But only in few of them the influence on the turbine dynamics produced by the interaction between mechanical and electrical parts of the HAWT is taken into account. Such an interaction is very essential for a so-called small-scale turbine with the generator connected to a local electrical circuit. Changes of electrical load influence such turbines greatly. In particular, the hysteresis of a trapped power with respect to increase/decrease of electrical load appears. This fact was shown for a classical (one propeller) HAWT in the frames of closed mathematical model by Dosaev et al. (2009).

In the current paper it is supposed that the generator of the double disk HAWT is connected to a local electrical circuit. The closed dynamical model with taking into account electromechanical interaction in the system is constructed. One of the parameters of the model is responsible for the value of external resistance in the circuit, so it describes the load from consumers upon the HAWT.

A special type of a double disk HAWT is studied: Propellers are installed at two rings of a differential planet gear (DPG), a rotor of a generator is connected to the third ring of the gear. Thus, the dynamics of the system essentially differs from that of a classical double disk HAWT, for which one propeller is joined to a rotor of a generator and the other is joined to a stator.

The evident advantage of using the DPG is that the relative angular speed of the rotor of the generator can be much higher than the relative angular speed of one propeller with respect to the other. Moreover, the DPG offers more options for additional control devices.

2 Description of the Mechanical System

The mechanical system includes two propellers. The front propeller is rigidly joined to the carrier of a DPG, the second propeller is rigidly joined to the external ring of the DPG (Figure 1). The front propeller is supposed to produce good torque at high tip speed ratio (to be leading at a regular mode of the operation). The back propeller is supposed to produce rather good torque at low tip speed ratio (to be leading at a starting stage of the operation). A rotor of a generator is rigidly joined to the sun gear of the DPG. The generator is connected to a local electrical circuit with a changeable external resistance.

Assume that r_c, r_s, r_r, r_p are the radiuses of corresponding rings, J_c, J_r, J_s, J_p are the central moments of inertia

of rigid bodies “front propeller + carrier”, “back propeller +external ring”, “sun + rotor”, each planet, m_p is the mass of each planet.

Suppose that there is no slipping between elements of DPG. Then the mechanical system has two degrees of freedom.

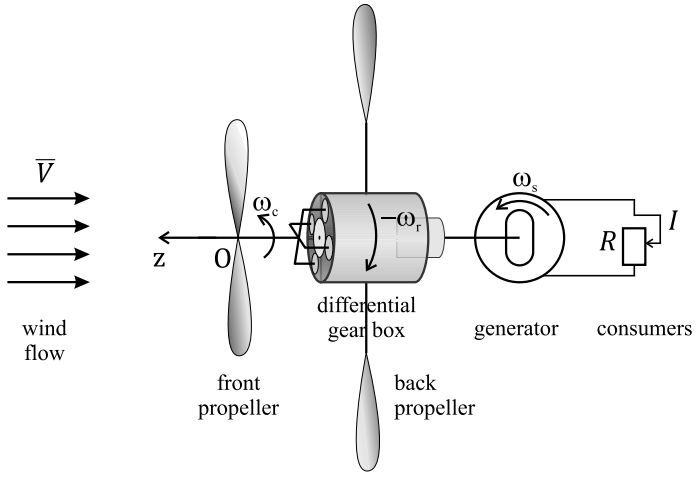

Figure 1. A general scheme of the system.

2.1 Model of External Forces

Assume that each propeller is under an aerodynamic action of an upcoming wind flow of a speed V, and the rotor of the generator is influenced by an electromagnetic field presenting between the rotor and the stator. Let us use the following model (similar to Dosaev et al. (2009, 2015)) for corresponding torques: Aerodynamic torques T_c , T_r and electromagnetic torque T_s with respect to the axis of rotation.

$$\begin{aligned} T_c &= 0.5\rho S b V^2 f_c(\lambda), \quad \lambda = b\omega_c V^{-1}, \\ T_r &= 0.5\rho S d V^2 f_r(\eta), \quad \eta = d\omega_r V^{-1}, \\ T_s &= -c^2\omega_s (R+r)^{-1}, \end{aligned} \tag{1}$$

where ω_c, ω_s, ω_r, are the angular speeds of the carrier, the sun, and the external ring of the DPG, b is the radius of the front propeller, d is the radius of the back propeller, S is the characteristic area of each propeller, ρ is the air density, λ and η are the tip speed ratio of the front and back propeller respectively, c is the coefficient of electromechanical interaction (responsible for conversion of mechanical energy into electrical energy), r is the inner resistance of the generator, R is its external resistance. $f_c(\lambda)$, $f_r(\eta)$ are dimensionless functions of an aerodynamic torque.

Examples of functions $f_c(\lambda)$, $f_r(\eta)$ are represented in the Figure 2. The qualitative behavior of these functions for $\lambda > 0$ and $\eta < 0$ respectively corresponds to results of experimental tests (see Dosaev et al. (2009)). Parts of the curves, for which $\lambda < 0$ and $\eta > 0$ respectively, correspond to non-desirable direction of the propeller rotation. It is supposed that in these cases the aerodynamic torque increases or decreases exponentially. Thus, the functions $f_c(\lambda)$, $f_r(\eta)$ are continuous, but not differentiable at $\lambda = 0$ and $\eta = 0$ respectively (Figure 2).

Further qualitative results are valid for a wide class of functions. For the front propeller, the product $\omega_c T_c$ is positive for $\lambda \in (0, \lambda_1)$ and for $\lambda \in (\lambda_2, \lambda_3)$. For the back propeller, the product $\omega_r T_r$ is positive for $\eta \in (\eta_1, 0)$. The maximum absolute value of aerodynamic torque for the front propeller is larger than that for the back one. Thus, if the front propeller starts from zero angular speed, it can not reach its optimal angular speed without external help. On the other hand, if the back propeller works alone, it can not produce as high torque as the maximum torque of the front one.

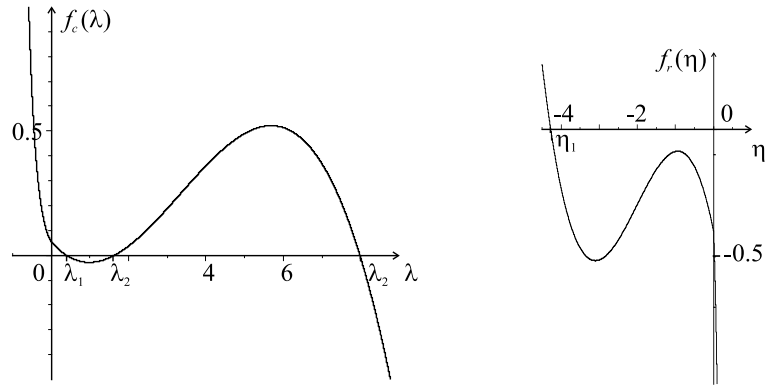

Figure 2. Dimensionless aerodynamic torques (on the same scale).

In further calculations it is assumed for simplicity that $b = d$ (the radius of the front propeller is equal to the radius of the back propeller).

3 Dynamical Equations and Statement of the Problem

Dynamical equations for a single-propeller HAWT with a DPG were derived in Dosaev et al. (2009). These equations can be easily modified for the case of two propellers, taking into account the relations (1). The obtained equations for a double rotor HAWT are as follows:

$$\begin{aligned} \lambda' &= a(A_2 + A_3)f_c(\lambda) + kA_3 f_r(\eta) - pa^{-1}A_2\lambda + pk^{-1}A_2\eta; \\ \eta' &= kf_c(\lambda) + k^2(a^{-1}A_3 + A_1)f_r(\eta) + pka^{-1}A_1\lambda + pA_1\eta, \end{aligned} \tag{2}$$

where

$$\begin{aligned} &p = \frac{c^2}{2(R+r)\rho S b^2 V}, \quad a = \frac{r_s}{4r_c}, \quad k = \frac{a}{1-2a}, \\ &A_1 = \frac{r_c}{Jr_s}\rho S b^3 (\frac{r_r r_p}{2r_c r_s}J_c + \frac{2r_c r_r r_p}{r_s}m_p - \frac{2r_c r_r}{r_s r_p}J_p), \\ &A_2 = \frac{r_c}{Jr_s}\rho S b^3 (\frac{r_p}{2r_r}J_r + \frac{r_r}{r_p}J_p), \\ &A_3 = \frac{r_c}{Jr_s}\rho S b^3 (\frac{r_r r_p}{2r_s^2}J_r + \frac{r_r}{r_p}J_p), \\ &J = \frac{r_p r_r J_c J_s}{4r_s^2} + \frac{r_p J_c J_r}{4r_r} + \frac{r_c^2 r_p J_s J_r}{r_s^2 r_r} + \frac{r_r J_c J_p}{r_p} + \frac{r_c^2 r_r J_s J_p}{r_s^2 r_p} + \frac{r_c^2 J_r J_p}{r_r r_p} + \frac{r_c^2 r_r J_s m_p r_p^2}{r_s^2 r_p} + \\ &+ \frac{r_c^2 J_r m_p r_p^2}{r_r r_p} + \frac{4r_c^2 r_r J_p m_p r_p^2}{r_p^3}. \end{aligned}$$

All listed parameters are positive values. Parameter p is responsible for the electrical load in the circuit and for the wind speed, parameters A_1 , A_2 , A_3 , J are responsible for geometrical and inertia properties of the system.

Stable steady solutions of the system (2) correspond to operation modes of the wind turbine.

The task is to describe these steady solutions depending on parameters of the model, especially with respect to the parameter p. This parameter is responsible for the changeable conditions of operation such as the wind speed and the external resistance (e.g. if there are no consumers in the circuit, p is zero). The other parameters of the model for a particular wind turbine are fixed. Another task is to design a control strategy that allows reaching the operation mode with maximal trapped power.

4 Operation Modes

Each steady solution (λ^*, η^*) of the system (2) satisfies the following equations:

$$\begin{aligned} \lambda' &= a(A_2 + A_3)f_c(\lambda) + kA_3 f_r(\eta) - pa^{-1}A_2\lambda + pk^{-1}A_2\eta = 0; \\ \eta' &= kf_c(\lambda) + k^2(a^{-1}A_3 + A_1)f_r(\eta) + pka^{-1}A_1\lambda + pA_1\eta = 0. \end{aligned} \tag{3}$$

Equations (3) define two curves: $\lambda' = 0$ and $\eta' = 0$. These curves divide the plane $\{\lambda, \eta\}$ into domains with determined signs of λ' and η'. Thus the direction of the trajectory $(\lambda(\tau), \eta(\tau))$ is determined in each domain. This is enough to find steady points and check their stability.

An example is shown in the Figure 3. The curve "1" is given by $\{\lambda' = 0\}$, the curve "2" is given by $\{\eta' = 0\}$; the arrows represent qualitative direction of trajectories in corresponding domains; black points correspond to attracting steady solutions, white points correspond to repelling steady solutions. The picture was constructed numerically for the following values of the parameters: $a = 0.125$, $A_1 = 3.7$, $A_2 = 2.8$, $A_3 = 3.4$, and $p = 0.0008$.

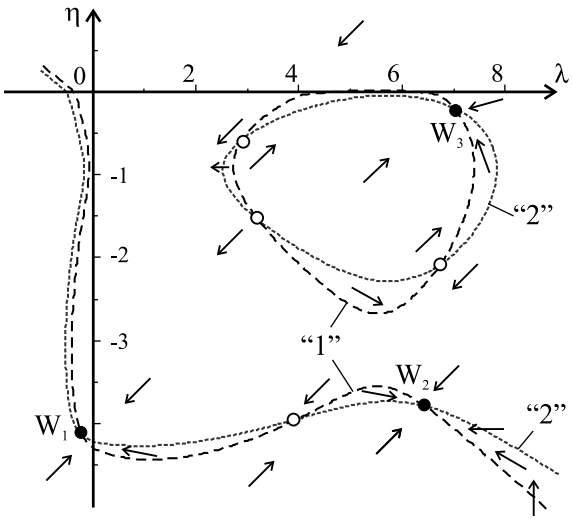

Figure 3. An example of location of steady points in the plane $\{\lambda, \eta\}$.

In our example the system possesses three attracting steady states: $W_i, i = 1, 2, 3$ (Figure 3).

In the operation mode corresponding to W_1 both propellers rotate in the same direction. The rotation speed of the back propeller is high, and the rotation speed of the front propeller is close to zero. In the operation mode corresponding to W_2 the propellers rotate in opposite directions with a rather high speed. In the operation mode corresponding to W_3 the propellers rotate in opposite directions, the speed of the front propeller is high, the speed of the back propeller is close to zero.

An attracting steady regime is preferable for practical applications, if a corresponding value $(\omega_c T_c + \omega_r T_r)$ of mechanical power taken from the flow is the largest. For the case shown in Figure 3, such a regime corresponds to the steady point $W_2 = \{\lambda^* = 6.4, \eta^* = -3.7\}$. Notice, that maximal value of $\lambda f_c(\lambda)$ could be reached for $\lambda = 6.2$, and maximal value of $\eta f_r(\eta)$ corresponds to $\eta = -3.4$. Thus, in the operation mode corresponding to the point W_2 , the power produced by both propellers is near the maximum. The value $p = 0.0008$ is chosen for the purpose to get closer to the maximum power taken from the flow.

5 Discussion and Control Strategy

The following problem is to reach a preferable operation mode from the starting state of the turbine, i.e. $\{\lambda = 0, \eta = 0\}$. For a single propeller small-scale HAWT, this problem can be solved by disconnecting consumers at the stage of starting the turbine (Dosaev et al. (2009)). Consumers are to be connected when the turbine reaches a rather high speed. This approach is suitable for a HAWT with aerodynamic torque function qualitatively similar to the function f_r in Figure 2 (the equation $f_r(\eta) = 0$ has only one root). But if the only propeller of a HAWT is qualitatively similar to the front propeller, no high angular speed can be expected without additional starter.

In our double disk system, the back propeller acts as a starter for the front one. Still from the Figure 3 one can notice that the point $\{0, 0\}$ doesn't belong to the domain of attraction of the preferable steady state W_2.

The following control strategy bringing the system to a preferable operation mode is proposed:

Step 1. The external load coefficient p is set to zero, that means the consumers are disconnected from the circuit of the generator. (This first step is similar to the case of a single propeller HAWT.) The system will go to the steady

state with small λ and rather high η (see Figure 4). All parameters of the model in Figure 4 are similar to those in Figure 3 except the value of external load coefficient p. Thus, Figure 4 characterizes the behavior of the same turbine for disconnected electrical load.

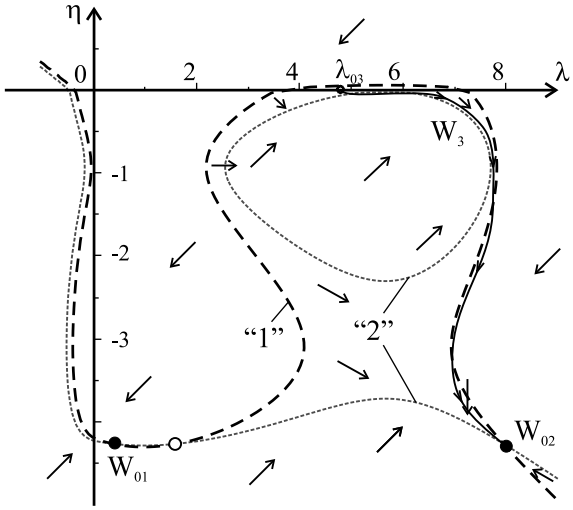

Figure 4. An example of location of steady points for $p = 0$. Solid line shows an example of a trajectory.

From zero initial conditions, the system approaches the attracting steady state W_{01}, that is approximately $\{0.4, -4.3\}$ in our example. If we just connect the desirable electrical load ($p = 0.0008$), the task will not be fulfilled, because the point W_{01} is not in the domain of attraction of W_2 (but in the domain of attraction of the state W_1). So additional step of control switching is needed.

Step 2. Let p be zero and the system be already in the state W_{01}. Apply the brake torque to the external ring. Here we assume that the brake system can be applied to any ring of the DPG, and it stops the corresponding ring very quickly. Additionally, assume that the moment of inertia of the sun ring is much higher than the moment of inertia of the carrier. So when the brake stops the external ring, the angular speed ω_s of the sun remains almost constant. Neglect small deviations of ω_s, and write down the kinematic relation ($\omega_s r_s = 2\omega_c r_c - \omega_r r_r$) before and after applying the brake:

$$\begin{aligned} &\omega_{s01} r_s = 2\omega_{c01} r_c - \omega_{r01} r_r, \\ &\omega_{s01} r_s = 2\omega_{c03} r_c. \end{aligned} \tag{4}$$

From equations (4) we obtain that the angular speed of the carrier after the second control intervention will be $\omega_{c03} = \omega_{c01} - 0.5\omega_{r01} r_r / r_c$. In our example $r_r / r_c = 2$. So we obtain: $\lambda_{03} = \lambda_0 1 - \eta_0 1 \approx 0.4 + 4.3 = 4.7$. Notice that for $\lambda \approx 4.7$, as well as for $\eta = 0$, the aerodynamic torque acting upon the corresponding propeller is accelerating (with respect to desirable direction of rotation). In our example for the case $p = 0$, the point $\{\lambda_{03}, 0\} \approx \{4.7, 0\}$ is in the domain of attraction of the point $W_{02} \approx \{8, -4.3\}$ (Figure 4). So after the system comes close to the state $\{\lambda_{03}, 0\}$ we switch off the brake, allowing the external ring to move free. Then the system moves from the state $\{\lambda_{03}, 0\}$ to the state W_{02}.

Step 3. Now the system is in the state W_{02}. Connect electrical load, making the desirable value $p = 0.0008$. For $p = 0.0008$, the point W_{02} is in the domain of attraction of the desirable steady point W_2. The task is fulfilled.

It is noticeable that for the classical double disk contra-rotating HAWT, for which one propeller is joined to a rotor of a generator and the other is joined to a stator, and no DPG is used, the problem of accelerating one propeller using another one has not such an easy solution. In that case there is no option for a brake to transmit the energy of rotation of one propeller into the energy of contra-rotation of the other without special additional mechanism.

Thus, we confirmed one of the advantages of a DPG, that is to offer useful control options for reaching the desirable operation modes.

6 Conclusions

In this paper the closed dynamical model of a double propeller contra-rotating HAWT with a DPG is introduced. Torsional behavior of the system under external loading is discussed. Steady operation modes are studied with respect to a certain example of the configuration of the system. By this example it is shown that the system possesses an operation mode for which mechanical power produced by each propeller is close to its maximum. To obtain such an operation mode certain conditions on parameters of the model should be fulfilled.

It is the common situation, that the domain of attraction of this desirable operation mode does not include the initial state of the system with zero angular speeds of both propellers. Due to this fact, the special control strategy that makes the system reach desirable operation mode is constructed. This strategy involves two control actions: Disconnection/connection of consumers in the local electrical circuit of the generator and switching on/off of the brake applied to the external ring of the DPG. It was shown on the example, that this strategy provides the desirable result.

References

Dosaev, M.; Holub, A.; Klimina, L.: Preferable operation modes of a wind turbine with a differential planetary gearbox. *Mech. Mach. Sci.*, 25, (2015), 545–552.

Dosaev, M.; Lin, C.-H.; Lu, W.-L.; Samsonov, V.; Selyutskii, Y.: A qualitative analysis of the steady modes of operation of small wind power generators. *J. Appl. Math. Mech.*, 73(3), (2009), 259 – 263.

Farthing, S.: Robustly optimal contra-rotating hawt. *Wind Engineering*, 34(6), (2010), 733–742.

Hansen, M.: *Aerodynamics of Wind Turbines*. Routledge, London and New York (2015).

Jung, S.; No, T.-S.; Ryu, K.-W.: Aerodynamic performance prediction of a 30kw counter-rotating wind turbine system. *Renew. Energy*, 30(5), (2005), 631–644.

Lee, S.; Kim, H.; Son, E.; Lee, S.: Effects of design parameters on aerodynamic performance of a counter-rotating wind turbine. *Renew. Energy*, 42, (2012), 140–144.

Shen, W.; Zakkam, V.; Sorensen, J.; Appa, K.: Analysis of counter-rotating wind turbines. *Journal of Physics: Conference Series*, 75(1), (2007), 1–9.

Address: 1, Michurinckiy prospect, Moscow, 119192, Russia
email: ekateryna-shalimova@yandex.ru, klimina@imec.msu.ru